

Excess Thermodynamic Properties of H₂O and D₂O Solutions of Tetramethylurea, an Azeotropic System. Vapor Pressures, Excess Vapor Pressures, and Vapor Pressure Isotope Effects

Gyorgy Jakli[†] and W. Alexander Van Hook^{*‡}

KFKI Atomic Energy Research Institute of the Hungarian Academy of Sciences, H-1525 Budapest, P.O.B. 49, and Chemistry Department, University of Tennessee, Knoxville, Tennessee 37996-1600

Vapor pressures of the tetramethylurea (TMU) + H₂O or + D₂O solutions (1, 2, 4, 8, 15, 25, 50, and 70 molal, 283 ≤ *T*/K ≤ 353) were obtained from precise differential measurements. The vapor pressures in the lower temperature range show sharp maxima that are 40 to 50% above the Raoult's law value at $X_{\text{TMU}} = 0.07$ (4 molal) which fall with increasing temperature. The vapor pressure isotope effects of the solutions lie significantly below that for pure solvent. Below 50 °C the difference shows its maximum at 2 to 4 aquamolal, reaching unusually large values at low temperature (40% at 10 °C). The behavior of the solution is discussed using the cage-model of hydrophobic hydration. In the water-rich region, competition between hydrophobic and hydrophilic hydration spheres results in unusually high TMU activity and solution nonideality and in turn accounts for the strong denaturing effect of TMU on natural proteins; this effect is most effective at about 3 *m*.

Introduction

Urea and its alkyl derivatives sometimes act as conformational perturbants and denaturing agents of aqueous polypeptides and protein solutions,^{1,2} and for that reason the structure of their aqueous solutions has been systematically studied.^{3,4} Denaturing by alkyl ureas is usually stronger than that for urea and increases with alkyl (apolar) content.⁵ While in many cases urea has a maximum denaturing effectiveness at 6 to 7 *m* (molal),⁶ the maximum was found around 5 *m* for 1,3-dimethylurea (DMU) and about 3 *m* for tetramethylurea (TMU).⁷ It is useful to ask whether the denaturing actions at these concentrations are caused by significant changes in solution structure induced by the ureas or rather are due to peptide–urea interactions not directly related to the changes in the solvent structure. It is in that context we engaged in a program of measurement of H₂O–D₂O solvent isotope effects on the thermodynamic properties of urea, 1,3-DMU, and TMU solutions over wide ranges of concentration and temperature.^{8–11} The properties investigated included excess free energies, enthalpies, and entropies of solution and apparent and partial molar volumes. So far as aqueous solutions of urea itself are concerned,^{8,9} the results can be rationalized using the idea that urea only slightly disturbs the water structure (by reducing the degree of water–water hydrogen bonding). It exhibits a monotonic “substitutional-type” behavior in solution, which results in no abrupt change in any of the properties investigated across the entire (wide) range of possible concentration. However, the volumetric properties of aqueous 1,3-DMU and TMU solutions show extrema when plotted against concentration,^{10–12} as is characteristic for the “interstitial-type” solution processes characteristic of polar organic compounds.¹³ Some have interpreted such

behavior by supposing that different (equilibrium) solution structures dominate above and below the extrema concentrations.

H₂O–D₂O solvent isotope effects on solution thermodynamics are useful in sorting out the different components of intermolecular interaction which occur in solution. The dielectric properties of H₂O and D₂O are closely matched and their ion–dipole and dipole–dipole solute–solvent interactions should be practically the same. On the other hand, at least at low temperature, D₂O is more structured than H₂O, and the properties of solutions in D₂O are more sensitive to changes in solvent–solvent interactions induced by the presence of the solute. In the qualitative interpretation of solvent isotope effects it is presumed that the changes in solvent–solvent interactions will dominate and the solute–solvent interactions largely cancel.

Experimental Section

Materials. Laboratory distilled water was treated with basic potassium permanganate and twice redistilled using an all-glass apparatus. Heavy water (Merck and Co., analytical grade) was used without further purification. D/H analysis, made using a Mettler-Paar densitometer, yielded $100[n_D/(n_D + n_H)] = (99.77 \pm 0.01)$ atom % D. Tetramethylurea (Merck, analytical grade) was freshly distilled under vacuum. H₂O and D₂O stock (“mother”) solutions of equal aquamolality ($m = (\text{mole of solute})/(\text{55.508 mol of solvent})$) were prepared and diluted gravimetrically as appropriate.

Differential Vapor Pressure Measurements. Vapor pressure differences between pure solvent and solutions or between normal and heavy water solutions of identical aquamolality were measured by differential capacitance manometry as previously described.^{14,15} In this technique the different samples are held in a thermostated block, whose temperature is controlled to within ±0.001 K and measured by platinum resistance thermometry to ±0.01

[†] KFKI Atomic Energy Research Institute of the Hungarian Academy of Sciences.

[‡] University of Tennessee.

Table 1. Parameters of Eq 1: $\ln(P/\text{kPa}) = A - B/[C + (T/^\circ\text{C})]$

m^a	A	B	C	$10^3\sigma$	no. of data pts
1 (H)	18.373 (0.25) ^b	5188 (151)	277 (4.5)	2.34	13
1 (D)	19.066 (0.36)	5583 (226)	285 (6.4)	3.22	13
2 (H)	20.346 (0.27)	6711 (203)	327 (5.7)	3.97	19
2 (D)	22.319 (0.30)	8222 (246)	364 (6.2)	3.65	19
4 (H)	22.146 (0.34)	8214 (283)	369 (7.2)	3.34	17
4 (D)	24.000 (0.49)	9757 (444)	403 (10)	4.16	17
8 (H)	19.465 (0.14)	5991 (99)	303 (2.9)	2.61	20
8 (D)	20.417 (0.23)	6621 (163)	318 (4.5)	3.78	20
15 (H)	17.894 (0.174)	4765 (105)	257 (3.3)	5.02	21
15 (D)	17.470 (0.073)	4471 (42)	245 (1.4)	2.31	21
25 (H)	16.701 (0.052)	4033 (28)	229.7 (0.94)	1.37	19
25 (D)	16.855 (0.068)	4072 (36)	227.7 (1.2)	1.83	19
50 (H)	16.203 (0.057)	3796 (30)	218.5 (1.0)	1.71	19
50 (D)	16.320 (0.066)	3813 (34)	215.9 (1.2)	2.01	19
70 (H)	16.084 (0.058)	3788 (30)	217.6 (1.0)	2.07	20
70 (D)	16.180 (0.065)	3795 (33)	214.8 (1.1)	2.36	20
TMU ^c	15.013 (0.175)	4052 (93)	219.5 (3.0)	8.61	23
H ₂ O ^c	16.635 (0.021)	4022 (12)	234.8 (0.40)	0.81	24

^a Molality (mol/(55.508 mol of solvent)). ^b Parenthesized figures are 1σ uncertainties. ^c 100%.

K. The precision for aqueous systems is about 0.2 to 0.3% of $\Delta P/P$ in the temperature range ($278 \leq T/\text{K} \leq 353$).

Results

Vapor Pressure and Vapor Pressure Isotope Effects.

Vapor pressures of normal water solutions (P_{H}^m) were obtained from the differential measurements, $\Delta P = P_{\text{H}}^\circ - P_{\text{H}}^m$, between pure water, P_{H}° , and solutions, P_{H}^m ($m = 1, 2, 4, 8, 15, 25, 50$, and $70 m$), at 2 to 3 K intervals for ($283 \leq T/\text{K} \leq 353$). P_{H}° is available at the experimental temperatures from the literature.¹⁵ To represent the data, least-squares fits were made with the Antoine equation

$$\ln(P/\text{kPa}) = A - B/[C + (T/^\circ\text{C})] \quad (1)$$

Fitting parameters, standard deviations, and the number of data points measured are reported in Table 1. Vapor pressure differences between H₂O and D₂O solutions, $\Delta P = P_{\text{H}}^m - P_{\text{D}}^m$, of identical aquamolality, $m = (\text{moles solute}/(55.508 \text{ mol solvent}))$, were used to obtain P_{D}^m .

$$P_{\text{D}}^m = P_{\text{H}}^{m,(1)} - \Delta P \quad (2)$$

where $P_{\text{H}}^{m,(1)}$ is the smoothed vapor pressure of the H₂O solution obtained from the fits to eq 1. P_{D}^m data from eq 2 have also been least-squares fitted to the Antoine equation, eq 1, and the parameters are included in Table 1. Using Table 1, P_{H}^m and P_{D}^m values have been calculated at rounded temperatures and plotted versus mole fraction of TMU, as shown in Figure 1. The plots show a pronounced maximum in the pressure (i.e. minimum boiling azeotrope) which develops in the low-temperature region around 4 m and then damps out as temperature increases.

In an alternate representation of the data we report the difference between the natural logarithms of the ratios of isotopic vapor pressures in pure solvent, $\ln R^\circ = \ln(P_{\text{H}}^\circ/P_{\text{D}}^\circ)$, and solution, $\ln R^m = \ln(P_{\text{H}}^m/P_{\text{D}}^m)$, in Table 2, given by

$$\Delta \ln R = \ln R^\circ - \ln R^m = \ln(P_{\text{H}}^\circ/P_{\text{D}}^\circ) - \ln(P_{\text{H}}^m/P_{\text{D}}^m) \quad (3)$$

$\Delta \ln R$ values were obtained from $\ln(P_{\text{H}}^m/P_{\text{D}}^m) = \ln(P_{\text{H}}^m/(P_{\text{H}}^m - \Delta P))$ using P_{H}^m from Table 1, and measured values of ΔP for each experimental temperature, together with

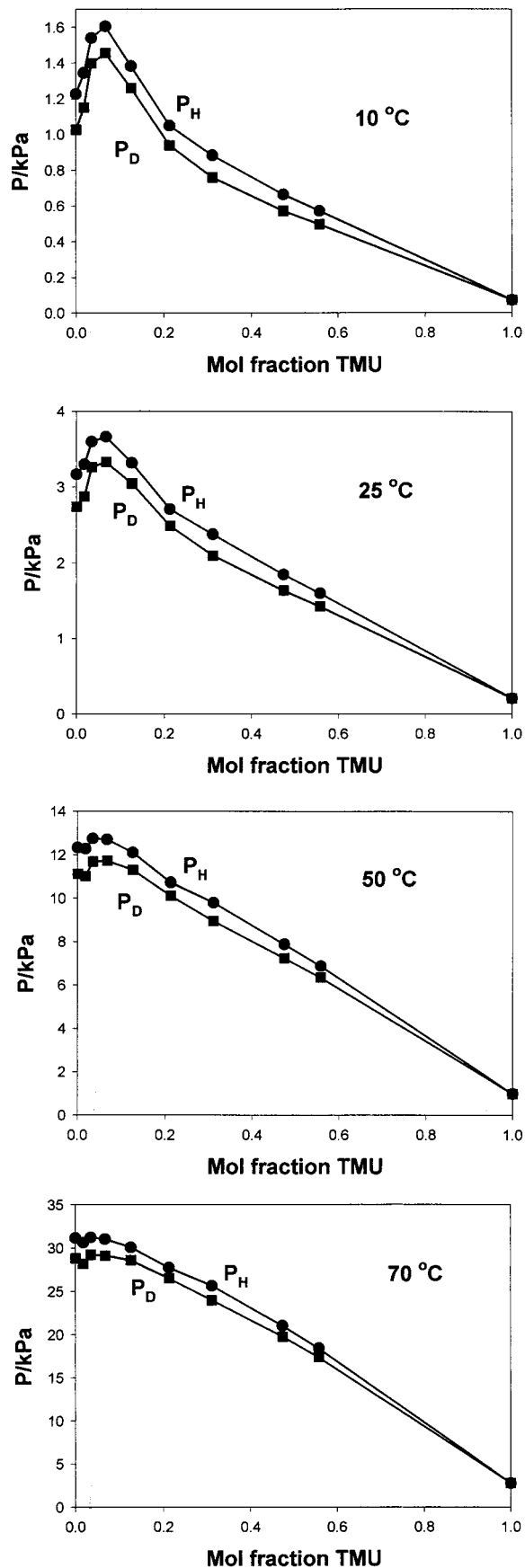


Figure 1. Vapor pressures of solutions of tetramethyl urea in H₂O and D₂O at four temperatures. Calculated from Table 1. The lines, drawn point to point, are guides to the eye. Upper curves (filled circles), TMU/H₂O; lower curves (filled squares), TMU/D₂O.

Table 2. Parameters of Eq 4: $\Delta \ln R = \ln(P_H^o/P_D^o) - \ln(P_H^m/P_D^m) = A_0 + A_1(T^\circ\text{C}) + A_2(T^\circ\text{C})^2 + A_3(T^\circ\text{C})^3$

m^a or X^b	$10^2 A_0$	$-10^3 A_1$	$10^5 A_2$	$-10^7 A_3$	$10^3 \sigma$
1/0.017 70	4.615 (0.154) ^c	1.736 (0.23)	2.423 (0.89)	1.232 (1.0)	1.26
2/0.034 75	9.619 (0.126)	3.169 (0.1)	3.622 (0.24)	1.406 (0.17)	0.68
4/0.067 16	9.562 (0.151)	3.382 (0.12)	4.284 (0.28)	1.887 (0.19)	0.65
8/0.125 94	7.802 (0.07)	2.6781 (0.06)	3.600 (0.15)	1.728 (0.11)	0.68
15/0.212 76	4.378 (0.05)	1.062 (0.05)	1.228 (0.12)	0.5468 (0.08)	0.50
25/0.310 66	3.268 (0.03)	0.7729 (0.03)	1.164 (0.07)	0.6825(0.05)	0.21
50/0.472 46	3.500 (0.03)	0.4942 (0.03)	0.5920 (0.07)	0.2993 (0.05)	0.21
70/0.557 83	3.838 (0.02)	0.4967 (0.02)	0.5376 (0.04)	0.2755 (0.03)	0.20

^a Molality (mol/(55.508 mol of solvent)). ^b Mole fraction. ^c Parenthesized figures are 1σ uncertainties.

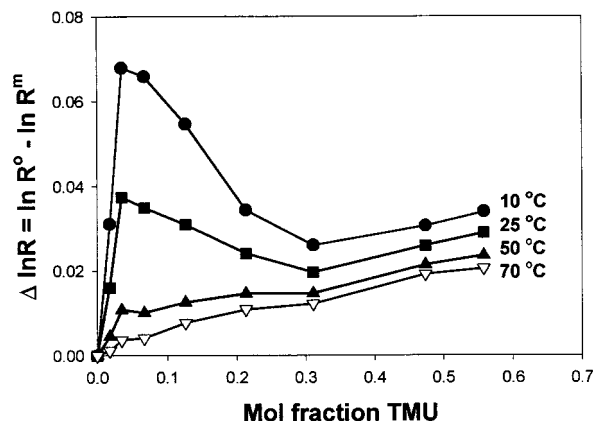


Figure 2. Vapor pressure isotope effects in the TMU/H₂O/TMU/D₂O system. $\Delta \ln R = \ln R^o - \ln R^m = \ln(P_H^o/P_D^o) - \ln(P_H^m/P_D^m)$. Calculated from Table 2. The lines, drawn point to point, are guides to the eye.

$\ln R^o$ values earlier determined by us on the same apparatus,¹⁶ were least-squares fitted to an empirically selected relation,

$$\Delta \ln R = A_0 + A_1(T^\circ\text{C}) + A_2(T^\circ\text{C})^2 + A_3(T^\circ\text{C})^3 \quad (4)$$

The parameters are reported in Table 2 (the number of $\ln R^m$ data points used to obtain these fits is the same as that for the fits reported in Table 1). $\Delta \ln R$ is shown as a function of temperature and concentration in Figure 2. As is to be expected, the extrema in the vapor pressures of the H₂O and D₂O solutions observed at low TMU concentration result in a similar pattern in the $\Delta \ln R$ plots (compare Figures 1 and 2). In an alternate representation of the vapor pressure isotope effect (VPIE) data we show plots of the deviation of the vapor pressures of TMU/H₂O and TMU/D₂O solutions from Raoult's law ($P^{\text{dev}}/\% = 100(P_m^{\text{TMU}} - P^o)/P^o$) in Figure 3. The maximum at about $m = 4$ remains apparent. The point of interest, nicely illustrated in this representation, is the inverse isotope dependence of the effect, $P^{\text{dev}}/\%(\text{TMU}/\text{D}_2\text{O}) > P^{\text{dev}}/\%(\text{TMU}/\text{H}_2\text{O})$.

Activity Coefficients (Approximation). The maxima in Figure 1 define azeotropic loci, where the concentration of each component is constrained to be the same in the liquid (X_i) and gas phases (Y_i). At this composition it is a simple matter to calculate the water (γ_w) and TMU (γ_{TMU}) activity coefficients neglecting corrections for nonideality in the vapor phase.

$$P_i = X_i \gamma_i P_i^o = Y_i P^m \quad (5)$$

$$\gamma_i = Y_i P^m / X_i P_i^o = P^m / P^o \quad (6)$$

In eqs 5 and 6, P_i is the partial vapor pressure of the i th component, P^o is the vapor pressure of the pure component,

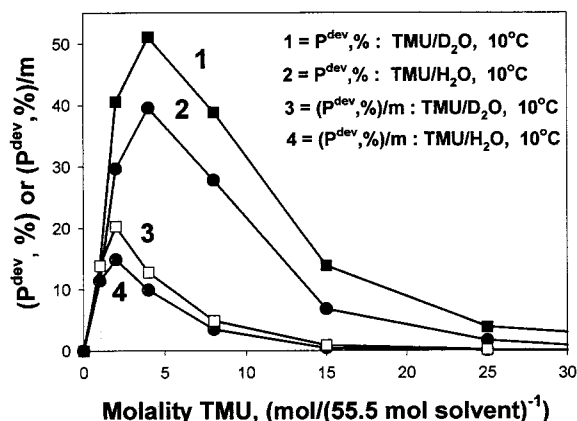


Figure 3. Relative vapor pressure deviations, $P^{\text{dev}}/\%$, and concentration weighted relative excess pressures, $(P^{\text{dev}}/\%)/m$, for the TMU/H₂O/TMU/D₂O system at 10 °C. $P^{\text{dev}}/\% = 100[P(\text{solution}) - P(\text{ideal, Raoult})]/[P(\text{ideal, Raoult})]$. Note the inverse isotope effect, $P^{\text{dev}}/\%(\text{TMU}/\text{D}_2\text{O}) > P^{\text{dev}}/\%(\text{TMU}/\text{H}_2\text{O})$. The lines, drawn point to point, are guides to the eye. Lower curves (filled circles), TMU/H₂O; upper curves (filled squares), TMU/D₂O.

and P^m is the (total) vapor pressure at the azeotropic concentration. That concentration is at or close to 4 m , but due to the uncertainty in precisely locating the maximum, and because we have neglected corrections for vapor nonideality, the activity coefficients at azeotropic composition (Figure 4) are approximate. A more thorough analysis of activity coefficients in TMU/H₂O/D₂O will be published separately.

Discussion

Among numerous investigations published on the solution thermodynamics of aqueous TMU solutions, only that of Lindfors and co-workers¹⁷ reports previous measurements of vapor pressure. Besides the vapor pressure (VP), those authors also investigated viscosity, density, surface tension, and heats of mixing. Because their VP study was carried out at 45 °C for ($0.1 \leq X_{\text{TMU}} \leq 1$), however, the VP maximum we report at $X_{\text{TMU}} = 0.07$ was not detected in their work. In fact, in the water-rich region ($X_{\text{TMU}} < 0.1$) they report extrema only for the heat of mixing, where a maximum was observed at $X_{\text{TMU}} = 0.07$. Nevertheless, they paid little attention to its location, noting only that the maximum is not necessarily indicative of formation of a TMU/water complex. A number of authors later reported various extrema in the water-rich region of aqueous TMU solutions. Thus, the partial molar volume versus concentration curve has a sharp minimum at $X_{\text{TMU}} = 0.03$ (2 m)¹⁸ and the ultrasonic sound-velocity (adiabatic compressibility) versus concentration curves (isotherms from 10 to 35 °C) also intersect at this concentration.^{18,19} This kind of behavior seems to be characteristic for aqueous solutions of larger polar organic molecules and has been rationalized using the Wen-Saito concept of "interstitial" solution

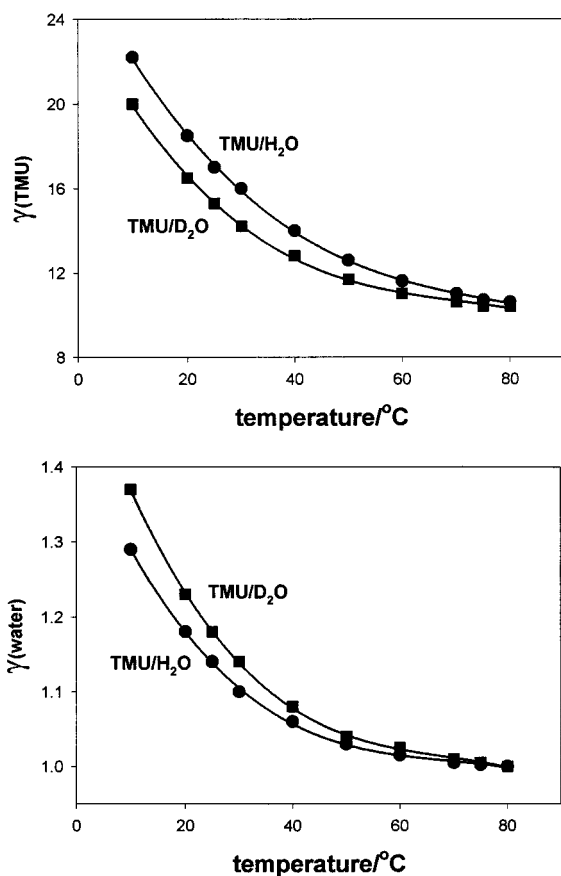


Figure 4. Approximate solute and solvent activity coefficients in the TMU/H₂O/TMU/D₂O system at the azeotropic compositions. For the Raoult's law reference state, see the text. Filled circles, TMU/H₂O solutions; filled squares, TMU/D₂O solutions.

(caging) of hydrophobic molecules.¹³ In that interpretation, it is supposed that all bulk water is hydrated at the concentration which defines the minimum in V_2 , and with further increase in concentration hydration spheres overlap more and more, and this leads to eventual collapse of the hydrophobic cage structure. A closer look at the present VP data shows that the VP maximum (azeotropic composition) of the TMU solutions corresponds to $X_{\text{TMU}} = 0.07$ (4 m). The vapor pressure deviation function ($P^{\text{dev}}/\% = 100 - (P_m^{\text{TMU}} - P^{\circ})/P^{\circ}$), that is, that fractional change in vapor pressure over and above the Raoult's law value, peaks at that concentration. Figure 3 illustrates the situation at 10 $^{\circ}\text{C}$. Here, in H₂O, P^{dev} peaks rather sharply near 4 m TMU, and the D₂O data behave similarly although $P^{\text{dev}}(\text{D}_2\text{O}) > P^{\text{dev}}(\text{H}_2\text{O})$. At this low temperature the enhancement is remarkably large, about 38% for H₂O and about 47% for D₂O solutions at 10 $^{\circ}\text{C}$ (Figure 3), and $\Delta \ln R/\ln R^{\circ} = 0.39$, but the effects dampen as temperature increases. Across the entire range of temperature, however, the relative effect is larger in D₂O, the more strongly structured solvent. This lends credence to the interpretation that it is hydrophobic structuring which dominates in determining the solution thermodynamics of these solutions at lower temperature and modest concentration.

One possible interpretation for both the excess vapor pressure and the vapor pressure isotope effect data employs the hydrophobic caging model. Three concentration regions are distinguished. Below 2 m Wen-Saito "caging" dominates and rapidly consumes "free" water, until at about 2 m (which is the concentration where $(P^{\text{dev}}/\%)/m$ peaks) essentially no "free" or "bulk" water remains. The region between about 2 and ~ 15 m is characterized by interaction

(overlapping) of the hydration spheres. At the maximum for $P^{\text{dev}}/\%$, about 4 m , the solute-solvent ratio is 1:14, while for the complete cage, at about 2 m , it is 1: 28. In the third region, $m > \sim 15$, structural considerations no longer dominate, but rather hydrogen bonding between the TMU and water becomes the most important interaction.

A weak interaction (repulsion) between TMU/water complexes (cages) centered on neighboring TMU's is expected on the basis of the "structural hydration interaction" model, proposed by Desnoyers and co-workers.²⁰ According to this line of thinking, an overlap of hydration spheres of the same type (hydrophobic/hydrophobic or hydrophilic/hydrophilic) results in a reenforcement of water clustering around the solute, but overlap of unlike hydration spheres centered on neighboring TMU's gives the opposite effect. High concentration forces unlike interaction, and this in turn causes a drop in P^{dev}/m from its maximum near 2 m to near zero around 15 m . Throughout the change, however, D₂O solutions remain the more highly structured. During the discussion one keeps in mind that in its direct interaction with water TMU acts only as an H-bond acceptor from water, never as a donor to water. This simple fact accounts for a large part of the difference in the thermodynamic properties of hydration in concentrated aqueous solutions of urea, 1,3-DMU (both of which act as both acceptor and donor), and TMU (acceptor only).

Literature Cited

- (1) Herskovits, T.; Gadegbeku, B.; Jailliet, H. On the Structural Stability and Solvent Denaturation of Proteins II. *J. Biol. Chem.* **1970**, *245*, 4544-4550.
- (2) Barone, G.; Galbiati, C.; Rizzo, E.; Volpe, V. Proceedings of the First European Biophysics Congress, Vol. 1, Baden, Vienna, 1971; p 49.
- (3) Barone, G.; Castronuovo, G.; Volpe, C. D.; Elia, V. NMR Studies of Aqueous Solutions of Alkylureas. Proton and Carbon-13 Chemical Shifts. *J. Solution Chem.* **1977**, *6*, 117-127.
- (4) Barone, G.; Castronuovo, G.; Cesaro, A.; Elia, V. Hydrophobic Effect in Aqueous Solutions of Nonelectrolytes II. Cross-Interactions of Alkylureas. *J. Solution Chem.* **1980**, *9*, 867-876 and references therein.
- (5) Barone, G.; Castronuovo, G.; Crescenzi, V.; Elia, V.; Rizzo, E. The Hydrophobic Effect in Aqueous Solutions of Nonelectrolytes. Self-interactions of alkyl ureas. *J. Solution Chem.* **1978**, *7*, 179-192.
- (6) Barone, G. Personal communication. 1997.
- (7) Herskovits, T.; Jailliet, H.; Desena, A. On the Structural Stability and Solvent Denaturation of Proteins III. *J. Biol. Chem.* **1970**, *245*, 6511-6517.
- (8) Jakli, Gy.; Van Hook, W. A. Isotope effects in aqueous systems. 12. Thermodynamics of Urea-*h*₂/H₂O and Urea-*d*₂/D₂O solutions. *J. Phys. Chem.* **1981**, *85*, 3480-3493.
- (9) Jakli, Gy.; Van Hook, W. A. Thermodynamic properties of solutions of urea, deuteriurea and tetramethylurea in H₂O and D₂O. *Stable Isot. Anal. Chem. Symp. Ser.* **1982**, *11*, 23-28.
- (10) Jakli, Gy.; Van Hook, W. A. H₂O-D₂O Solvent Isotope Effects on Apparent and Partial Molar Volumes of 1,3-Dimethylurea and Tetramethylurea Solutions. *J. Chem. Eng. Data* **1996**, *41*, 249-253.
- (11) Jakli, Gy.; Van Hook, W. A. Isotope Effects in Aqueous Systems. Excess thermodynamic properties of 1,3-dimethylurea solutions in H₂O and D₂O. *J. Chem. Eng. Data* **1997**, *42*, 1274-1279.
- (12) Phillip, P. R.; Perron, G.; Desnoyers, J. E. Apparent molal volumes and heat capacities of urea and methyl-substituted ureas in H₂O and D₂O at 25 $^{\circ}\text{C}$. *Can. J. Chem.* **1974**, *52*, 1709-1713.
- (13) Wen, W. Y.; Saito, S. Apparent and partial molal volumes of five symmetrical tetraalkylammonium bromides in aqueous solution. *J. Chem. Phys.* **1964**, *68*, 2639-2644.
- (14) Pupezin, J.; Jancso, G.; Van Hook, W. A. A System for Determinations of Precise Vapor Pressure Differences from -20 to 110 $^{\circ}\text{C}$, Including Temperature Control to 0.001 $^{\circ}\text{C}$ over that Range. *Isotopenpraxis* **1970**, *9*, 319-322.
- (15) Goff, J. A. In *Humidity and Moisture*; Wexler, A., Ed.; Reinhold: New York, 1963; Vol. 3, p 289.
- (16) Jakli, Gy.; Van Hook, W. A. Vapor Pressure of Heavy Water from 283 to 363 K. *J. Chem. Eng. Data* **1981**, *26*, 243-245.

- (17) Lindfors, K. H.; Opperman, S. H.; Glover, M. E.; Seese, J. D. Intermolecular Hydrogen Bonding. I. Effects on the Physical Properties of Tetramethylurea–Water Mixtures. *J. Phys. Chem.* **1971**, *75*, 3313–3316.
- (18) Sasaki, K.; Arakawa, K. Ultrasonic and Thermodynamic Studies of the Aqueous Solutions of Tetramethylurea. *Bull. Chem. Soc. Jpn.* **1973**, *46*, 2738–2741.
- (19) Jakli, Gy.; Baranowski, A.; Jerie, K.; Glinski, J.; Orzechowski, K. Positron Annihilation and Adiabatic Compressibility of Tetramethylurea Aqueous Solution. A Quasichemical Interpretation. *Bull. Pol. Acad. Sci. Chem.* **1994**, *42*, 7181–7185.
- (20) Desnoyers, J. E.; Arel, M.; Perron, G.; Jolicoeur, C. Apparent Molal Volumes of Alkali Halides in Water at 25 °C. Influence of Structural Hydration Interactions on the Concentration Dependence. *J. Phys. Chem.* **1969**, *73*, 3346–3351.

Received for review November 22, 2000. Accepted March 22, 2001. Support from the Ziegler Research Fund, University of Tennessee, and the Hungarian Research Fund (OTKA-1846) is acknowledged.

JE000362M